Supporting Information

Boutin et al. 10.1073/pnas.1404988111

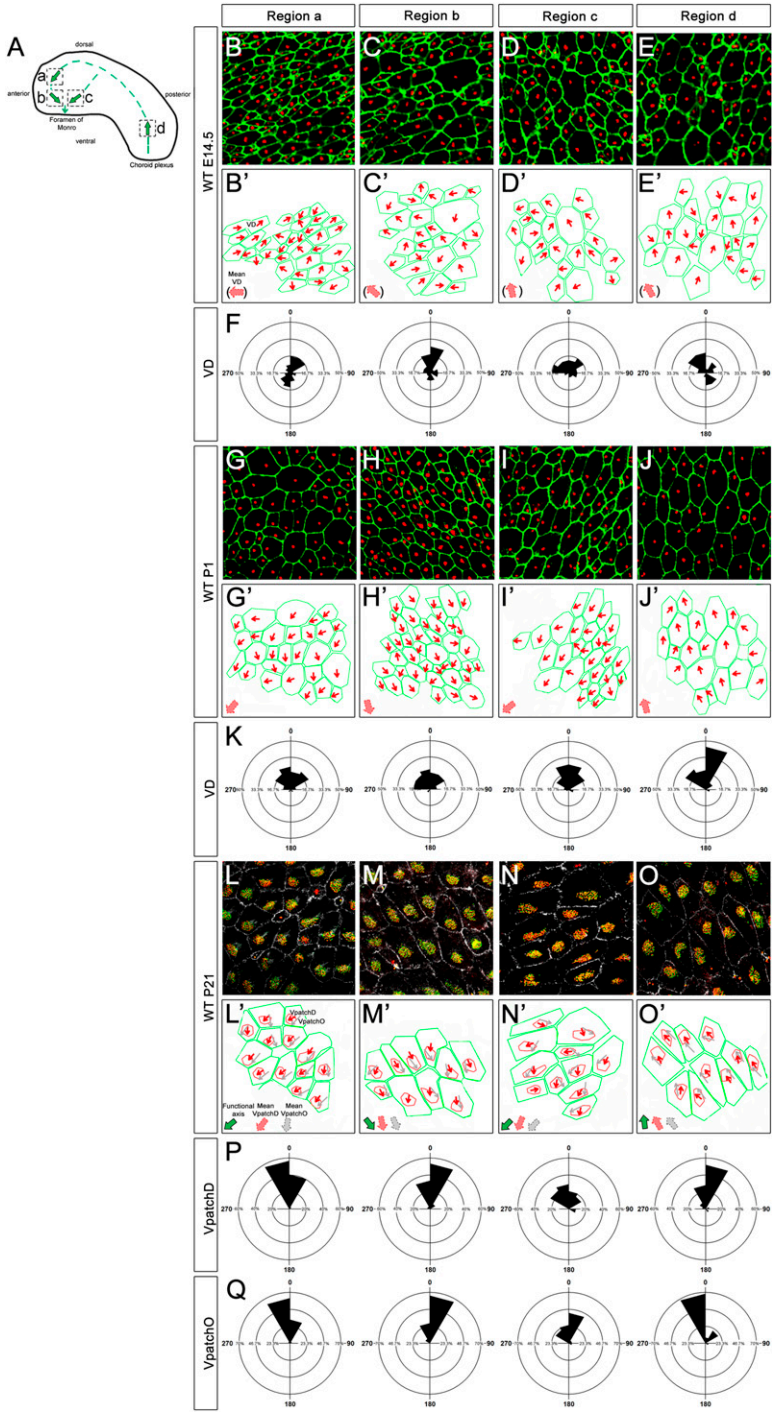

Fig. S1. Tissue polarity during lateral wall (LW) development. (*A*) Scheme depicting the four regions analyzed. Dashed green lines delineate the overall pattern of cerebrospinal fluid (CSF) circulation from the choroid plexus to the foramen of Monro. Thick green arrows outline the local directions of CSF movement (functional axis). (*B–J*) LW of WT (*B–E*) embryonic day (E) 14.5 and (*G–J*) postnatal day (P) 1 mice stained for ZO1 (green) and γ-tubulin (red). (*B′–E′* and *G′–J′*) Trace of the cell contour (green) in *B–J*. Red arrows represent vectors of basal body (BB) displacement (VD). Thick red arrows represent the mean VD. (*F* and *K*) Circular dispersion around the mean of vectors of displacement at (*F*) E14.5 and (*K*) P1. BB displacement is uncoordinated at E14.5, with vectors widely distributed around the mean in the four regions. At P1, a tissue-wide polarity is evidenced by the coordination of BB displacement and angular deviations

Legend continued on following page

mainly comprised between –45° and +45°. (*L–O*) LW of P21 WT mice stained for ZO1 (white), γ-tubulin (red), and FOP (green). (*L′–O′*) Trace of the cell contour (green) and BB patches (red) in *L–O*. Green arrows, functional axis; red arrows, VpatchD; thick gray arrows, mean VpatchO; thick red arrows, mean VpatchD; thin gray arrows, VpatchO. (*P* and *Q*) Circular dispersion around the mean of (*P*) VpatchD and (*Q*) VpatchO. In all regions, tissue-wide polarity of ependymal cells is evidenced by the coordination of VpatchD and VpatchO and low angular deviation of these vectors from the respective mean. In a given region, mean VpatchD and VpatchO directions always coincide with that of the functional axis. (Scale bar: *B–E*, 10 μm; *G–O*, 20 μm.)

Fig. S2. Cadherin, EGF-like, laminin G-like, seven-pass, G-type receptor (Celsr) 2 mutant mice. (*A*) Genomic organization of the *Celsr2* locus. The *Celsr2* gene is composed of 34 exons (black boxes). The null allele ($Celsr2^{-/-}$) was obtained by crossing floxed and PGK-Cre lines (*Materials and Methods*). (*B*) RT-PCR analysis of P1 brain extracts from WT and $Celsr2^{-/-}$. A 841-bp-long fragment, corresponding to nucleotides 3412–4252 [Geninfo identifier: 24475635; exons 2–4 (E2–E4); black arrows in *A*], was amplified in WT but not $Celsr2^{-/-}$ extracts.

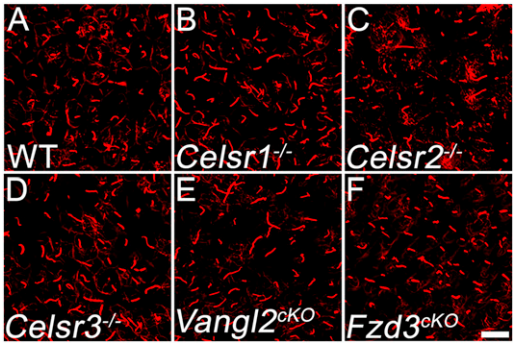

Fig. S3. Primary cilia develop normally in planar cell polarity (PCP) mutant mice. LW whole mounts from (*A*) WT, (*B*) $Celsr1^{-/-}$, (*C*) $Celsr2^{-/-}$, (*D*) $Celsr3^{-/-}$, (*E*) *Van Gogh like2*^{cKO} ($Vangl2^{cKO}$), and (*F*) *Frizzled 3*$^{-/-}$ ($Fzd3^{-/-}$) newborn mice stained with acetylated α-tubulin. Primary cilia are detected in all genotypes. (Scale bar: 10 μm.)

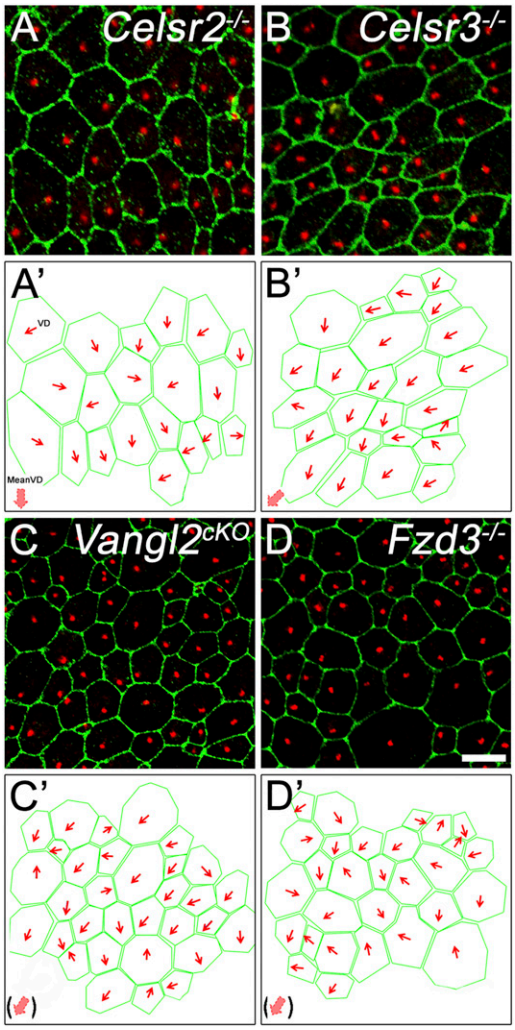

Fig. S4. Polarity of radial glia in *Celsr2*$^{-/-}$, *Celsr3*$^{-/-}$, *Vangl2*^{cKO}, and *Fzd3*$^{-/-}$ mice. Immunostainings of BB (γ-tubulin; red) with outline of the cell border (ZO1; green) and cilia polarity (red arrows) in (*A* and *A*′) *Celsr2*$^{-/-}$, (*B* and *B*′) *Celsr3*$^{-/-}$, (*C* and *C*′) *Vangl2*^{cKO}, and (*D* and *D*′) *Fzd3*$^{-/-}$ mutant radial glia (RG) cells. (*A*–*B*′) In *Celsr2*$^{-/-}$ and *Celsr3*$^{-/-}$, the BB positioning is coordinated between cells. (*C*–*D*′) In *Fzd3*$^{-/-}$ and *Vangl2*^{cKO}, the polarity of RG cells is disturbed. Red arrows, BB displacement; thick red arrows, mean displacement. (Scale bar: 10 μm.)

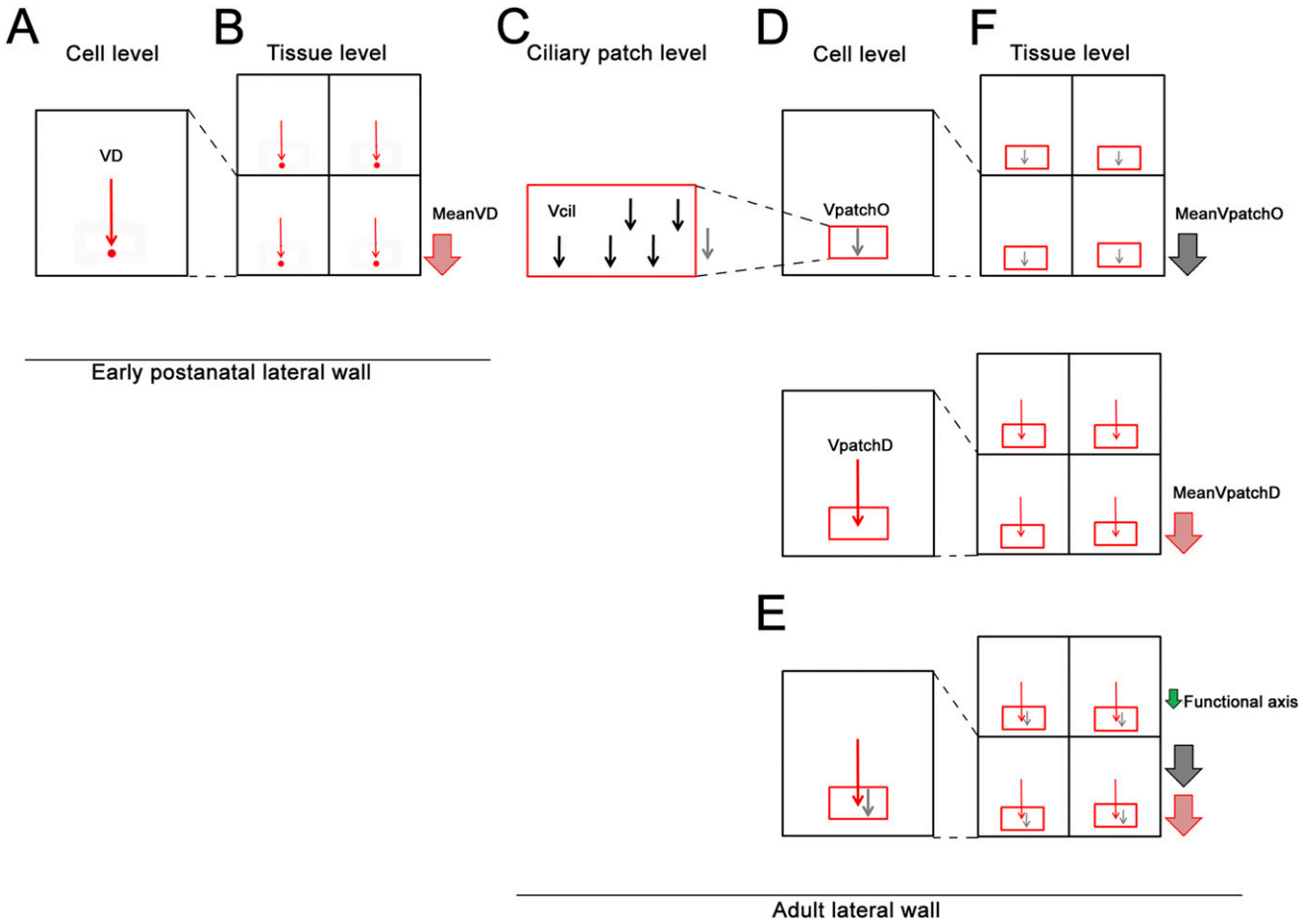

Fig. S5. Parameters to assess cilia polarity. (*A*–*E*) Schematic representation of parameters analyzed in (*A* and *B*) early postnatal RG and (*C*–*E*) adult ependymal cells. Red dots depict primary cilia, and red rectangles depict cilia patches. (*A* and *B*) In RG cells, the direction of the primary cilium displacement is shown by vector (VD) from the center of the apical surface to the primary cilium BB (red arrows). Coordination of BB displacement is evaluated by calculating the angle between individual vectors to the mean of the field (thick red arrow). (*C*) In ependymal cells, at the patch level, individual BBs orientation is defined by the vector Vcil (black arrows), and the coordination of Vcil is evaluated by the circular SD for individual patches. (*D*) At the cell level, two vectors define the polarity of ependymal cells. First, the mean Vcil or VpatchO (gray arrow) indicates the overall orientation of the patch and is the end result of rotational polarity. This vector also indicates the beating direction of a given cell. Second, VpatchD, related to translational polarity, is directed from the center of the apical surface to the center of the patch and defines the direction of patch displacement (red arrow). (*E*) In a given cell, these vectors are coincident. This intracellular coordination of patch orientation and displacement is evaluated by measuring the angle between VpatchD and VpatchO. (*F*) At the tissue level, LW polarity is reflected by similar directions of VpatchDs and VpatchOs in neighboring cells. In a given region, the mean VpatchO (thick gray arrow) and the mean VpatchD (thick red arrow) are parallel to each other and the direction of CSF circulation (functional axis; green arrow).

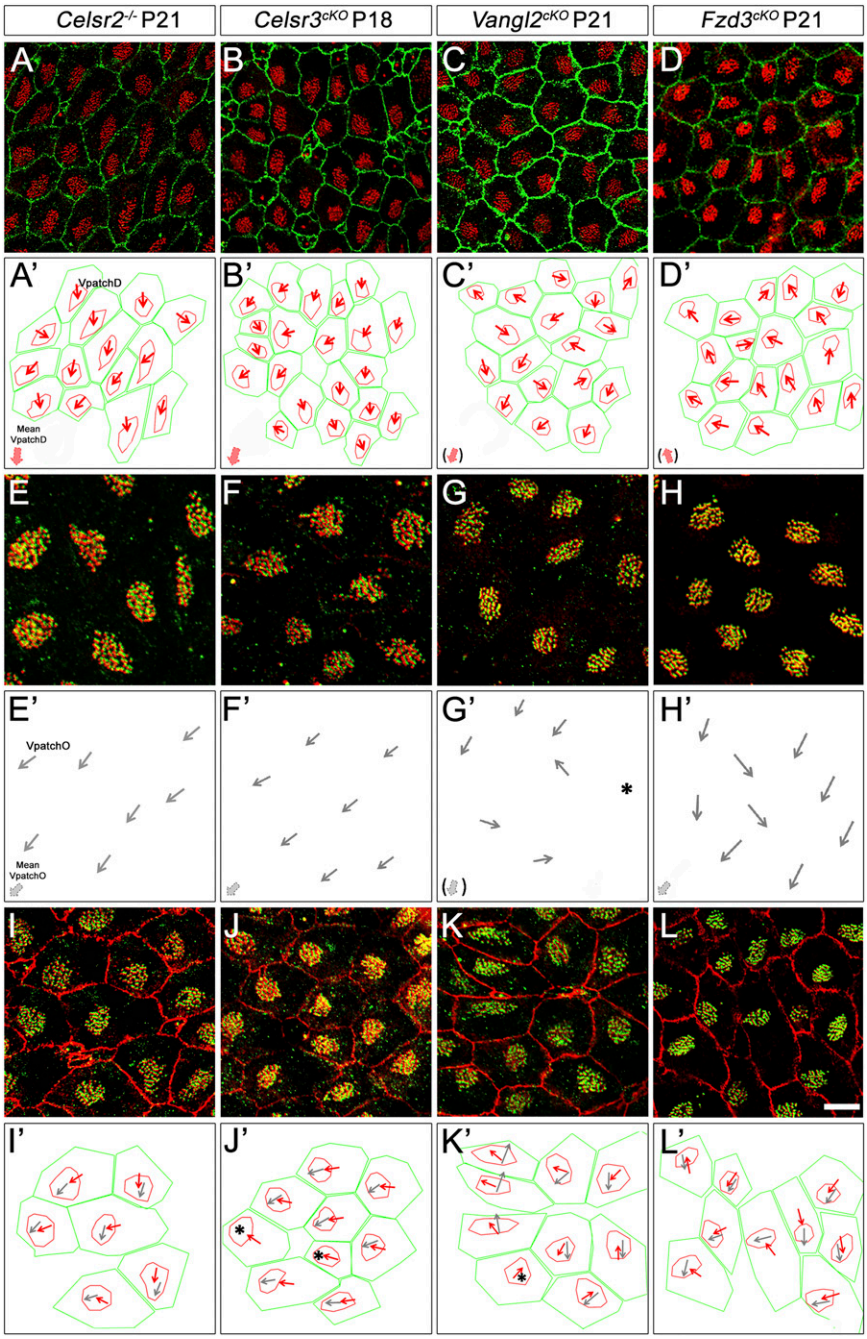

Fig. S6. Polarity of ependymal cells in *Celsr2*$^{-/-}$, *Celsr3*^{cKO}, *Vangl2*^{cKO}, and *Fzd3*^{cKO} mice. Immunostainings of BBs with outline of the cell border and cilia polarity (arrows), illustrating the planar polarity of ependymal cells in *Celsr2*$^{-/-}$ (column 1), *Celsr3*^{cKO} (column 2), *Vangl2*^{cKO} (column 3), and *Fzd3*^{cKO} (column 4) mutants. (*A*–*D*′) In all mutants, BBs patches are displaced from the center of the apical surface. (*A*–*B*′) In *Celsr2*$^{-/-}$ and *Celsr3*^{cKO}, patch positioning is coordinated between cells, whereas (*C*–*D*′) in *Fzd3*^{cKO} and *Vangl2*^{cKO}, this polarity is disturbed. (*E*–*H*) In the majority of individual mutant cells, BBs have the same orientation. (*E*–*F*′, *H*, and *H*′) In *Celsr2*$^{-/-}$, *Celsr3*^{cKO}, and *Fzd3*^{cKO}, patch orientation is coordinated between cells, whereas (*G* and *G*′) this polarity is disturbed in *Vangl2*^{cKO}. (*K*–*L*′) Intracellular coincidence of displacement and orientation is altered in *Fzd3*^{cKO}and *Vangl2*^{cKO}. Red arrows, VpatchD; small gray arrows, VpatchO; thick gray arrows, mean VpatchO; thick red arrows, mean VpatchD. *A cell with circular SD higher than 40° and ignored for VpatchO. (Scale bar: *A*–*D*, 5 μm; *E*–*H*, 10 μm; *I*–*K*, 15 μm.)

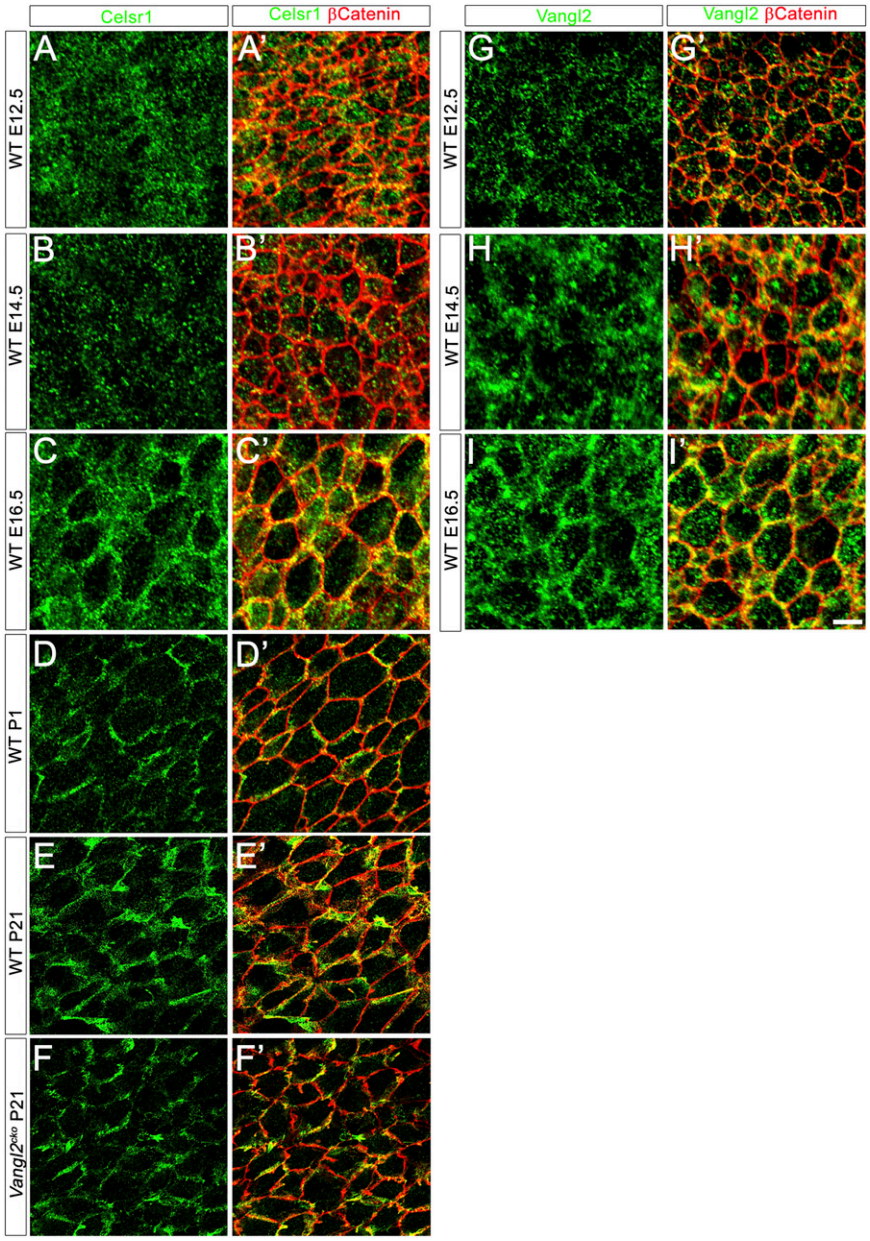

Fig. S7. Distribution of Vangl2 and Celsr1 proteins during ependymal development. (*A*–*E*′) WT and (*F* and *F*′) *Vangl2*^{cKO} LW at (*A* and *A*′) E12.5, (*B* and *B*′) E14.5, (*C* and *C*′) E16.5, (*D* and *D*′) P1, and (*E*–*F*′) P21 stained for (*A*–*F*) Celsr1 (green) and (*A*′–*F*′) β-catenin (red; merged in *A*′–*F*′). (*G*′–*I*′) LW from WT at (*G* and *G*′) E12.5, (*H* and *H*′) E14.5, and (*I* and *I*′) E16.5 stained for (*G*–*I*) Vangl2 (green) and (*G*′–*I*′) βCat (red; merge in *G*′–*I*′). During embryonic development, no asymmetry of Celsr1 and Vangl2 is observed. A first bias in Celsr1 localization is observed in a subset of cells at (*D* and *D*′) P1 and becomes evident at (*E* and *E*′) P21. (*F* and *F*′) The coordinated localization of Celsr1, observed in WT tissue (*E* and *E*′), is impaired in *Vangl2*^{cKO}. (Scale bar: *A*–*D*′ and *G*–*I*′, 5 μm; *E*–*F*′, 10 μm.)

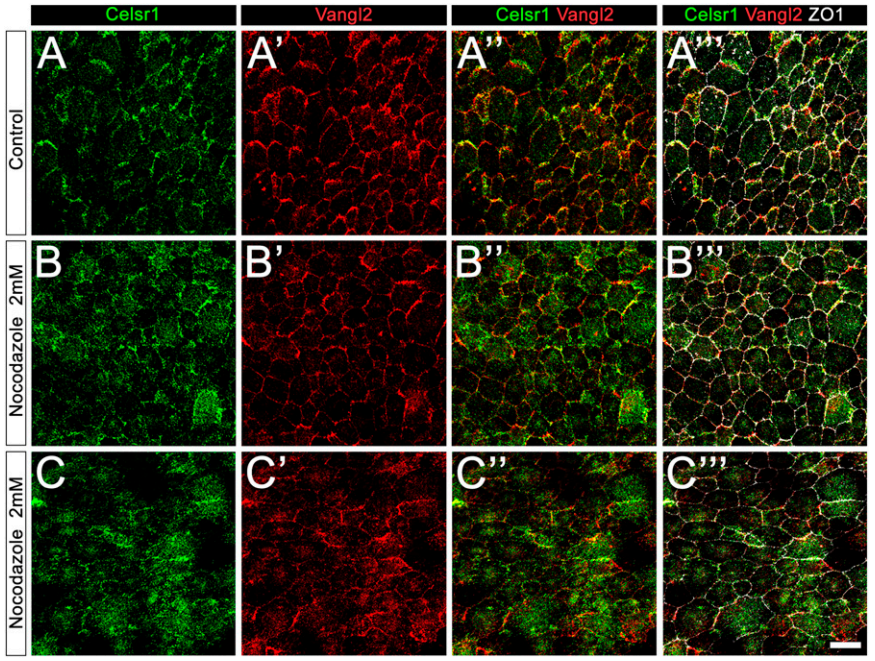

Fig. S8. Nocodazole treatment impairs Celsr1 and Vangl2 distribution at the cell membrane. LW 2 d postinjection of (*A*–*A*‴) control or (*B* and *C*‴) 2 mM Nocodazole solution stained for (*A*–*C*) Celsr1 (green) or (*A*′–*C*′) Vangl2 (red) and merged in *A*″–*C*″ or merged with ZO1 (white) in *A*‴–*C*‴. In controls (DMSO-injected animals; $n = 5$), asymmetric localization of Celsr1 and Vangl2 is observed. This distribution is impaired in the presence of Nocodazole. (Scale bar: 10 μm.)